

## EFFECT OF LOCAL ENERGY SUPPLY TO A HYPERSONIC FLOW ON THE DRAG OF BODIES WITH DIFFERENT NOSE BLUNTNES

V. Yu. Borzov, I. V. Rybka, and  
A. S. Yur'ev

UDC 532.5:532.135

*Parameters of the axisymmetric flow around bodies with different bluntness are compared in the case of constant energy supply to the main hypersonic flow. Flow structures, drag coefficients, and expenditure of energy on overcoming drag are analyzed with the effect of thermal energy on the flow taken into account for different bodies with equal volume.*

Results of many recent theoretical and experimental studies of super- and hypersonic flows around bodies that have a layer with a lower density [1-7] show that aerodynamic properties can be changed substantially by controlling the flow around the bodies by means of thermal energy supplied to the main flow. However, the great majority of the studies were carried out with a fixed shape of the bodies in the flow. This was usually a sphere [3] or a cylinder with a flat front face [4, 6]. In these studies either the geometric parameters were not changed at all or only the ratio of the dimensions of the region of energy supply to those of the body were changed or the distance between this region and the body was changed. At the same time, a comparative analysis of the flow around different bodies with thermal energy supply to the main flow is of practical interest.

With this in view, a numerical study of axisymmetric flow around bodies of revolution with the elliptical generatrix was carried out, varying with length of the semiaxis of the  $\xi$  ellipse located along the flow being varied (Fig. 1).

The initial system of equations is unsteady-state Euler equations for a compressible ideal gas in cylindrical coordinates  $(x, r)$ :

$$\frac{\partial \sigma}{\partial t} + \frac{\partial a}{\partial x} + \frac{\partial b}{\partial r} = -\frac{f}{r}, \quad (1)$$

where

$$\sigma = \begin{bmatrix} \rho \\ \rho u \\ \rho v \\ e \end{bmatrix}, \quad a = \begin{bmatrix} \rho u \\ p + \rho u^2 \\ \rho uv \\ (e + p)u \end{bmatrix}, \quad b = \begin{bmatrix} \rho v \\ \rho uv \\ p + \rho v^2 \\ (e + p)v \end{bmatrix}, \quad f = \begin{bmatrix} \rho v \\ \rho uv \\ \rho v^2 \\ (e + p)v \end{bmatrix};$$

$$e = \rho \left( \varepsilon + \frac{u^2 + v^2}{2} \right); \quad p = (\kappa - 1) \varepsilon \rho.$$

Conditions of absence of flow on the symmetry axis and on the body surface were prescribed. Derivatives of all parameters with respect to the coordinate  $x$  on the right-hand boundary of the calculation region were prescribed to be zero. On the other boundaries the flow was assumed to be undisturbed. These conditions were also used as initial conditions throughout the calculation region. When introducing the dimensionless variables, the

---

A. F. Mozhaisky Military Space Engineering Academy, St. Petersburg, Russia. Translated from *Inzhenerno-Fizicheskii Zhurnal*, Vol. 67, Nos. 5-6, pp. 355-361, November-December, 1994. Original article submitted July 22, 1993.

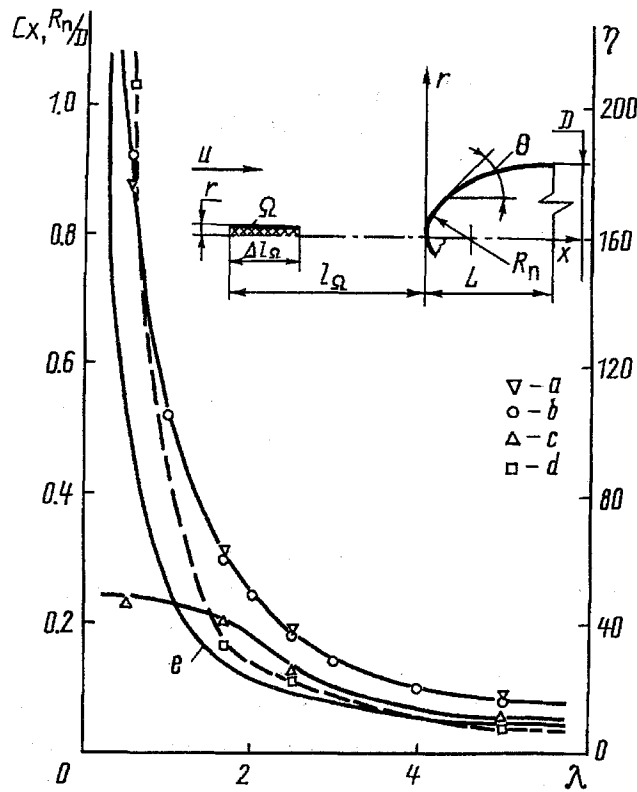


Fig. 1. Calculation scheme and plots of the drag coefficient  $C_x$  (a–c), the index of efficiency of the energy supply  $\eta$  (d), and the nose bluntness radius at the front point  $R_n$  (e) versus the aspect ratio of the nose  $\lambda$ ; a)  $C_x$  in the undisturbed main flow (calculation by S. K. Godunov's method); b)  $C_x$  in the undisturbed main flow (calculation by Newton's method); c)  $C_x$  in the flow controlled by energy supply (calculation by S. K. Godunov's method).

length  $D$  of the axis of the ellipse perpendicular to the flow was used as a scale of linear dimensions (Fig. 1). The velocity and density of the undisturbed flow were also used as scales. It was assumed that the energy was supplied to the thin cylindrical region  $\Omega$ , whose axis coincides with the symmetry axis of the body (Fig. 1). Geometric parameters and the rate of energy supply were determined from a series of calculations for a body with the aspect ratio  $\lambda = L/D = 1.67$ . For this body, in the case of the distance of the leading edge of the region from the body  $L_\Omega = 3D$ , its length  $\Delta l_\Omega = D$ , and its radius  $r_\Omega = 0.025D$ , the integral dimensionless rate of energy supply over the volume of  $\Omega$

$$\bar{I} = \frac{2I}{\rho_\infty u_\infty^3 S} = 3 \cdot 10^{-3}$$

provides a decrease in the drag coefficient  $C_x$  from 0.306 to 0.209 at the value of the main flow velocity corresponding to the Mach number  $M_\infty = 10$ . In what follows, when the aspect ratio  $\lambda$  is varied in the range 0.5–5, the other parameters were assumed constant. The energy supply was included in the initial system of equations (1) as the term in the right-hand side of the energy equation, corresponding to the energy supply  $q$  to unit volume per unit time. In accordance with the adopted dimensions of the region  $\Omega$  and value of  $\bar{I}$

$$q = 0.6 \rho_\infty u_\infty^3 / D.$$

Outside the region  $\Omega$ ,  $q = 0$ .

The initial system of differential equations (1) was approximated by a difference scheme, using S. K. Godunov's explicit scheme of first order of accuracy [8]. A stationary grid with the variable step in space and a

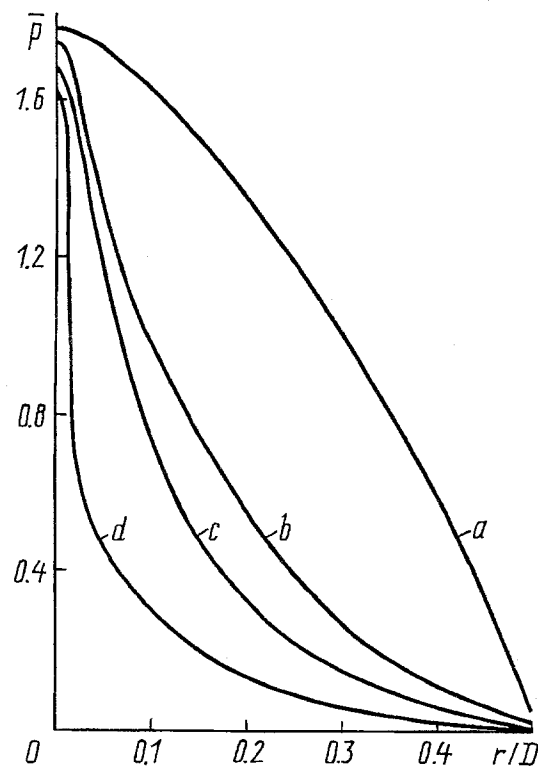


Fig. 2. Distribution of the pressure coefficient  $\bar{p}$  on the surface of the elliptic nose along the radial coordinate  $r$  for various aspect ratios  $\lambda$  with undisturbed flow around the body: a)  $\lambda = 0.5$ ; b) 1.67; c) 2.5; d) 5.

total number of cells of 2400 was used. Energy supply to the region  $\Omega$  was prescribed only after a steady solution was obtained for the flow around the body without energy supply. In the course of finding solutions the dynamics of the transition from one steady-state flow to another and back was traced.

Calculation results obtained with the above technique for the case of no energy supply are quite trivial as regards the flow structures and the distribution of gasdynamic parameters. Figure 2 shows distributions of the pressure coefficient  $\bar{p} = 2(p - p_\infty)/(\rho_\infty u_\infty^2)$  along the generatrix for bodies with an aspect ratio  $\lambda = 0.5, 1.67, 2.5,$  and 5 versus the radial coordinate  $r$ . In this case the integral characteristics, in particular, the drag coefficient  $C_x$ , are in good agreement with well-known data [9]. This is illustrated by comparison of the data of the numerical simulation (see Fig. 1a) with the results predicted by Newton's modified theory (Fig. 1b).

With energy supply the flow pattern changes substantially. While in the region  $\Omega$  itself and especially in its front part changes in the flow structure are determined just by thermal energy supply, the effect of the body on the distribution of gasdynamic parameters becomes more pronounced farther downstream. In the cases under consideration this effect is directly related to the bluntness radius in the neighborhood of the front critical point (Fig. 1e). For a body with an elliptic generatrix the local curvature radius at this point is defined by

$$R_n = D/4\lambda.$$

The presence of a region of energy supply with the aforementioned geometry and energy parameters gives rise to a long narrow channel in the flow with a decreased Mach number and density (about  $0.2\rho_\infty$ ). The transverse dimensions of this channel are commensurable with the radial dimensions of the region  $\Omega$ , while its length is many times greater than the chosen scale of linear dimensions. In the external part of the channel the gas acquires a small radial velocity component and its density increases slightly. By itself this restructuring of the flow is favorable for the flow around bodies with different bluntness radii in that it decreases the drag coefficient  $C_x$  (Fig. 1c). However, with the same expenditure of energy, the decrease in the drag coefficient is greater for bodies with a larger bluntness radius and a correspondingly smaller  $\lambda$ . This is clearly illustrated by the plot of the efficiency of

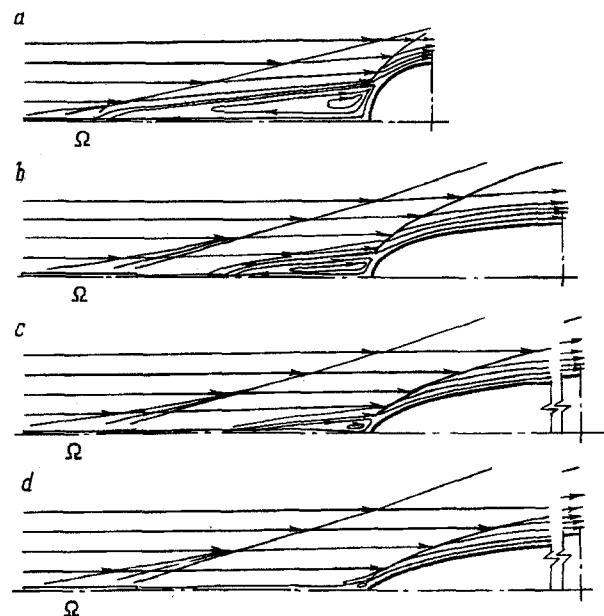
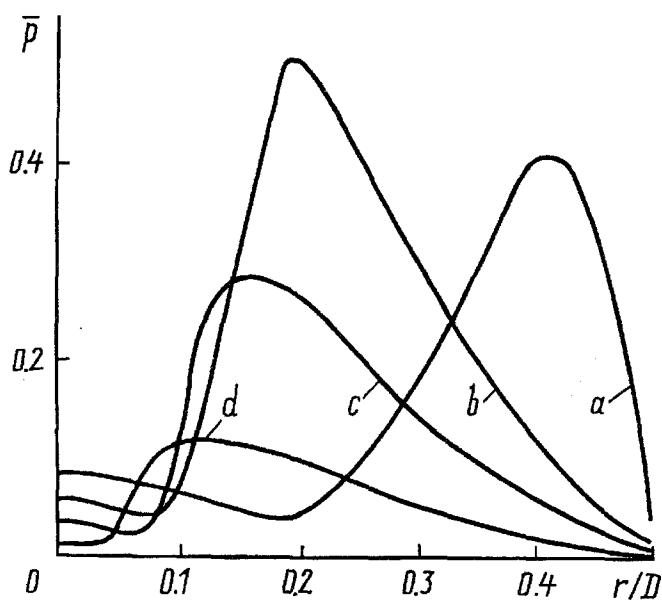


Fig. 3. Distribution of the pressure coefficient  $\bar{p}$  on the surface of the elliptic nose along the radial coordinate  $r$  for various aspect ratios  $\lambda$  with the flow controlled by energy supply: a)  $\lambda = 0.5$ ; b) 1.67; c) 2.5; d) 5.

Fig. 4. Gas flow around the front surface of bodies with various nose bluntness for the flow controlled by thermal energy supply: a)  $\lambda = 0.5$ ; b) 1.67; c) 2.5; d) 5.

energy supply  $\eta$  (Fig. 1d) versus the aspect ratio. The index  $\eta$  is the ratio of the change in the energy consumed per unit time to overcome the drag to the rate of the energy supply  $I$ :

$$\eta = \frac{\Delta X u_\infty}{I},$$

where  $\Delta X$  is the decrease in the drag when the flow around the body is controlled by energy supply. This behavior of the function  $\eta(R_n)$  is explained by the fact that at large bluntness radii the mentioned nonuniformity in the main flow gives rise to a substantial positive pressure gradient on the body surface in the radial direction. Near the front surface a separation zone is formed, the growth of which is favorable for additional restructuring of the flow and for a shift of the pressure maximum on the body surface in the direction of increase of the radial coordinate. However, in this case the pressure peak decreases as the local angle  $\theta$  between the generatrix and the flow at the boundary of the separation zone diminishes (Fig. 1). As a result, the pressure maximum and, consequently, the transverse dimensions of the separation zone correspond to  $\theta$  of at least  $40-45^\circ$ . This also means that the radial dimension of the region of reduced pressure in the neighborhood of the front point is limited and depends substantially on  $R_n$ , which is confirmed by the curves of the pressure coefficient on the body surface versus the radial coordinate shown in Fig. 3. Not only the transverse but also the longitudinal dimensions of the separation zone and even the possibility of its appearance depend on the ratio of the radial dimension of the region  $\Omega$  to the bluntness radius  $R_n$ . This is illustrated by the schematic flows shown in Fig. 4. The data presented in Figs. 3 and 4 correlate well with the results obtained in [6], where the ratio of the radial dimension of the region of energy supply to that of a cylinder with a flat front face was varied.

The above facts show that for bodies with a large bluntness radius of their noses, the energy supply provides a greater decrease in the drag coefficient relative to its value in the undisturbed flow at a higher efficiency  $\eta$ . Thus, a choice of parameters of energy supply that is based on  $R_n$  and data obtained for flow around a body with spherical bluntness ( $\lambda = 0.5$ ) seems more favorable as regards  $\eta$ . When this approach is used for the bodies considered at  $\lambda = 5$  ( $R_n = 0.05D$ ), the linear dimension of the region of energy supply becomes ten times smaller and the integral

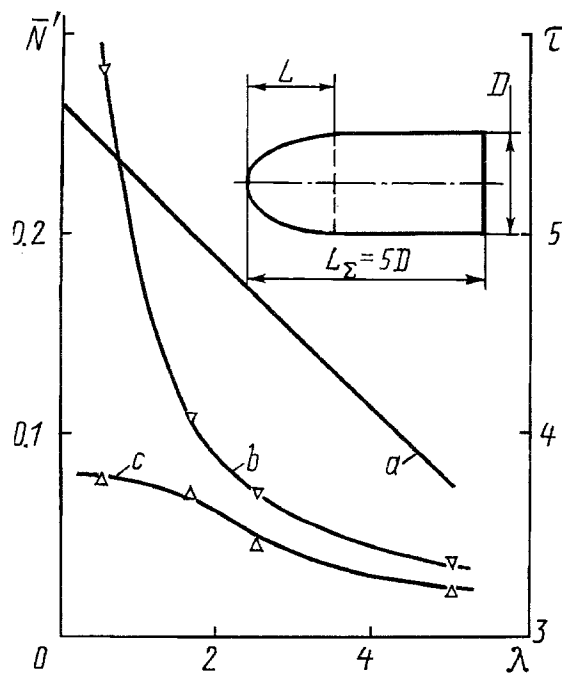


Fig. 5. Plots of the volume ratio (a) and the dimensionless expenditure of energy for overcoming the drag (b, c) versus the aspect ratio  $\lambda$  of the elliptic nose for bodies with the same aspect ratio  $\lambda_{\Sigma} = 5\lambda$ .

rate of energy supply decreases by two orders of magnitude. In this case even with the assumption that the radial dimension of the region where the energy supply affects the flow pattern is bounded by  $R_n$ ,  $\eta$  will correspond to the value obtained for the flow around a body with spherical bluntness, i.e., it increases from 8 to 207. However, the drag coefficient will decrease by just 0.006, while initially a value of 0.023 was obtained. In view of the drastic difference in two main indices characterizing the method of controlling the flow around a body by energy supply, the criterion  $\bar{N}$  defined as the ratio of the total rate of energy consumption to the rate in the undisturbed flow through the characteristic area of the body  $S$

$$\bar{N} = \frac{Xu_{\infty} + I}{\frac{3}{\rho_{\infty}u_{\infty}^3/2S}} = Cx + \bar{I}.$$

seems more acceptable for the choice of parameters of the energy supply and for comparison of characteristics of different bodies under these conditions.

Moreover, because of a substantial difference in the shape of the bodies considered, in comparing the characteristics, it is reasonable to add a cylinder to their tail part to achieve a total aspect ratio  $\lambda_{\Sigma} = 5$  (Fig. 5). In this case the comparison is of greater practical interest, and the differences in the components of the drag induced by friction and neglected in the calculations become insignificant. The line  $a$  in Fig. 5 shows the change in the volume ratio

$$\tau = V/S^{3/2},$$

where  $V$  is the volume of a body of revolution consisting of an elliptic nose and a cylinder. Then the dimensionless expenditure of energy for overcoming the drag of bodies with different nose bluntness and the same volume  $V$  is defined by

$$\bar{N}' = \frac{Xu_{\infty} + I}{\frac{3}{\rho_{\infty}u_{\infty}^3/2V^{2/3}}} = (Cx + \bar{I})/\tau^{2/3}.$$

Curve  $b$  in Fig. 5 shows  $\bar{N}'$  as a function of the aspect ratio of the nose of a composite body without energy supply and curve  $b$  is the same plot with constant parameters of energy supply described earlier. The shape of the curves shows that in the case of flow control by thermal energy supply the expenditure of energy for overcoming the drag decreases substantially and the effect of the nose bluntness on the energy consumption becomes less pronounced. A still greater decrease in the energy consumption can be achieved by purposeful optimization of the parameters of energy supply for each particular bluntness shape.

## NOTATION

$L$ , length of the ellipse semiaxis located along the flow;  $t$ , time;  $x, r$ , coordinates;  $\rho$ , density;  $P$ , pressure;  $u, v$ , components of the velocity vector;  $e$ , energy of unit volume of gas;  $\varepsilon$ , internal energy of unit mass of gas;  $w$ , velocity of gas;  $\kappa$ , adiabatic index;  $D$ , length of the ellipse axis normal to the flow;  $\Omega$ , region of energy supply;  $\lambda$ , aspect ratio of the ellipse;  $l_{\Omega}$ , distance between the front edge of the region of energy supply and the body;  $\Delta l_{\Omega}$ , length of the region of energy supply;  $r_{\Omega}$ , radius of the region of energy supply;  $I$ , integral (over the volume of the region  $\Omega$ ) rate of energy supply;  $\bar{I}$ , dimensionless rate of energy supply;  $S$ , characteristic area of the body;  $C_x$ , drag coefficient of the body;  $M$ , Mach number;  $R_n$ , bluntness radius of the body;  $\eta$ , index of the energy efficiency of the flow control;  $X$ , drag;  $\Delta X$ , decrease in the drag when the flow is controlled by energy supply;  $\theta$ , angle between the generatrix and the flow at the boundary of the separation zone;  $V$ , volume of the body;  $\tau$ , volume ratio of the body. Subscript  $\infty$  refers to the undisturbed flow.

## REFERENCES

1. S. I. Arafailov, *Izv. Akad. Nauk SSSR, Mekh. Zhidk. Gaza*, No. 4, 178-184 (1987).
2. V. I. Artem'ev, V. I. Bergel'son, A. A. Kalmykov, et al., *Izv. Akad. Nauk SSSR, Mekh. Zhidk. Gaza*, No. 2, 158-162 (1988).
3. P. Yu. Georgievskii and V. A. Levin, *Pis'ma Zh. Tekh. Fiz.*, 14, No. 8, 684-687 (1988).
4. V. I. Artem'ev, V. I. Bergel'son, I. V. Nemchinov, et al., *Izv. Akad. Nauk SSSR, Mekh. Zhidk. Gaza*, No. 5, 146-151 (1989).
5. L. V. Gogish and S. G. Dashevskaya, *Izv. Akad. Nauk SSSR, Mekh. Zhidk. Gaza*, No. 3, 180-183 (1990).
6. V. Yu. Borzov, I. V. Rybka, and A. S. Yur'ev, *Inzh.-Fiz. Zh.*, 62, No. 2, 243-247 (1992).
7. V. Yu. Borzov, I. V. Rybka, and A. S. Yur'ev, *Inzh.-Fiz. Zh.*, 63, No. 6, 659-694 (1992).
8. S. K. Godunov, A. V. Zabrodin, M. Ya. Ivanov, et al., *Numerical Solution of Multidimensional Problems of Gas Dynamics* [in Russian], Moscow (1976).
9. L. D. Grozdovskii (ed.), *Aeromechanics of Supersonic Flows around Bodies of Revolution of Power Shape* [in Russian], Moscow (1975).